Detecting surface runoff location in a small catchment using distributed and simple observation method

Judicael Dehotin, Pascal Breil, Isabelle Braud, Alban de Lavenne, Mickael Lagouy, Benoit Sarrazin

Detecting surface runoff location in a small catchment using distributed and simple observation method

Judicaël DEHOTIN[(1,5)], Pascal BREIL[1], Isabelle BRAUD[1], Alban de LAVENNE [(2,3)], Mickaël. LAGOUY[1], Benoît SARRAZIN[4]

1 Irstea, Centre de Lyon-Villeurbanne, 5 rue de la Doua CS70077 69626 VILLEURBANNE, France (jdehotin@gmail.com Tel. +33 06 52 62 74 03)

2 INRA, UMR1069, Soil Agro and HydroSystem, F-35000 Rennes, France,

3 AGROCAMPUS OUEST, UMR1069, Soil Agro and hydroSystem, F-35000 Rennes, France,

4 Université de Lyon ISARA-Lyon Agrapole, 3, rue Jean Baldassini 69364 LYON CEDEX 07 France

5 SNCF-INFRA PSIGT-LVE-EGP, 6, avenue François Mitterrand - 93574 La Plaine Saint Denis

ABSTRACT

Surface runoff is one of the hydrological processes involved in floods, pollution transfer, soil erosion and mudslide. Many models allow the simulation and the mapping of surface runoff and erosion hazards. Field observations of this hydrological process are not common although they are crucial to evaluate surface runoff models and to investigate or assess different kinds of hazards linked to this process. In this study, a simple field monitoring network is implemented to assess the relevance of a surface runoff susceptibility mapping method. The network is based on spatially distributed observations (nine different locations in the catchment) of soil water content and rainfall events. These data are analyzed to determine if surface runoff occurs. Two surface runoff mechanisms are considered: surface runoff by saturation of the soil surface horizon and surface runoff by infiltration excess (also called hortonian runoff). The monitoring strategy includes continuous records of soil surface water content and rainfall with a 5 minutes time step. Soil infiltration capacity time series are calculated using field soil water content and *in situ* measurements of soil hydraulic conductivity. Comparison of soil infiltration capacity and rainfall intensity time series allows detecting the occurrence of surface runoff by infiltration-excess. Comparison of surface soil water content with saturated water content values allows detecting the occurrence of surface runoff by saturation of the soil surface horizon. Automatic records were complemented with direct field observations of surface runoff in the experimental catchment after each significant rainfall event. The presented observation method allows the identification of fast and short-lived surface runoff processes at a small spatial and temporal resolution in natural conditions. The results also highlight the relationship between surface runoff and factors usually integrated in surface runoff mapping such as topography, rainfall parameters, soil or land cover. This study opens interesting prospects for the use of spatially distributed measurement for surface runoff detection, spatially distributed hydrological models implementation and validation at a reasonable cost.

Keywords*: Surface runoff, flooding, soil saturation, infiltration, sensor, field measurement*

1. INTRODUCTION AND CONTEXT

Heavy or long lasting rainfall events may trigger surface runoff and induce major flood hazards, even far from river networks. In France flooding by surface runoff represents 43% of flooding recognized as natural disaster (Dehotin and Breil, 2011a). This statistic was obtained using 140,000 natural disaster declarations in the French official national database since 1983. Thus surface runoff appears as one major cause of flooding in France, the other one being flooding by river overflow.

Surface runoff generation is a topic addressed by many authors in various research fields. These researches include for example understanding of surface runoff processes in various natural contexts (Lange and Haensler, 2012; Latron and Gallart, 2008; Muñoz-Villers and McDonnell, 2012; Wemple and Jones, 2003) or evaluating the role of surface runoff in pollution transfer or soil erosion (Beven, 2006; Bryan, 2000; Carey and Simon, 1984; El Kateb et al., 2013; Hudson, 1993; Wu et al., 1993). Several authors focused on the role of different landscape factors (microtopography, roughness, vegetation, land use, antecedent soil water content, water table, soil water potential etc.) and rainfall characteristics (rainfall intensities, drop size, storm kinetic energy etc.) on surface runoff generation (Arnaez et al., 2007; Braud et al., 2001; Castillo et al., 2003; Dunjó et al., 2004; Dunne et al., 1991; Dutton et al., 2005; Lafforgue, 1977; Latron and Gallart, 2008; Nicolas, 2010). Hydraulic features designing in engineering is also a domain for surface runoff investigation, mainly for evaluating surface runoff discharge, velocity or water depth (Boughton and Droop, 2003; Chanasyk et al., 2003; Jain and Singh, 2005; Koutroulis and Tsanis, 2010). Flood forecasting, groundwater recharge and irrigation are other topics of surface runoff survey (Harbor, 1994). There are two main approaches for surface runoff study and prediction: modeling-based and field observation-based methods.

Several models are used for surface runoff processes simulation or mapping. The Lisem model simulates surface runoff and rill erosion (De Roo et al., 1996a; De Roo et al., 1996b). The WEP and the RUSLE models (Nearing et al., 1989), are based on universal equation of soil losses (Renard et al., 1991). The RuiCells® model uses cell automaton method for surface runoff simulation (Douvinet et al., 2006; Langlois and Delahaye, 2002). These models are based on infiltration estimation combined with the overland kinematic wave equation to compute runoff discharge. Their parameterization or calibration can be performed using field experimentation (Connolly et al., 1997; Connolly and Silburn, 1995; Smith et al., 2004; Wu et al., 1993). Soil erosion mapping models are based on combinations of landscape factors such as soil type, land use and several topographic parameters (de Jong van Lier et al., 2005; Le Bissonnais et al., 1998; Le Gouée and Delahaye, 2008; Renard et al., 1991). Other models, like KINEROS2 (Smith et al., 1995; Woolhiser D.A. et al., 1990) and SEAGIS (DHI, 2002)

are designed to simulate sediment yield time series and the effect of management strategies to limit the erosion process. These models need field parameters such as distributed soil parameters or agricultural practices that are difficult to obtain. Moreover, the temporal dynamics of field parameters are generally not measured nor taken into account.

Field observations of surface runoff are usually achieved using various techniques. One of the most used is rainfall simulation devices (Abudi et al., 2012; Hartanto et al., 2003; Navas et al., 1990; Nicolas, 2010; Pérez-Latorre et al., 2010; Roose, 1977; Roose et al., 1993; Silva and Oliveira, 1999; Singh et al., 1999). It consists in field simulation of rainfall events with various intensities at fixed plots or using a mobile simulator. They allow estimating the rate of rainfall which infiltrates the soil and the one which flows overland. This technique allows testing the impact of different and realistic rainfall intensities. Nevertheless results are different from those of natural rainfall conditions because rainfall spatial heterogeneity is not integrated and soil initial conditions are not realistic for all simulations. Several field observation studies are based on tracer experiments. They use dye tracers or natural water isotopes ($\delta^{18}O$ of precipitation and stream waters) for chemically based hydrograph separations (Holzmann and Sereinig, 1997; Weiler et al., 1999). These experiments sometimes show the role of event water on surface runoff flow (Holzmann et al., 1997; Weiler et al., 1999). However meaningful identification of flow components and their generation mechanisms by these techniques needs coupling with other field data (Rice and Hornberger, 1998). These field experiment techniques of surface runoff observation are often heavy to install, to monitor and also difficult to replicate (installation and maintenance). Because the usual techniques are generally of large dimension and need specific skills, their deployment and monitoring on several sites are difficult. Usually they do not provide usable information about surface runoff mechanisms (Hudson, 1993). They are seldom used for validation purposes, to understand the role of several parameters on surface runoff processes or for soil parameters estimation in hydrological models. Thus existing observation techniques are not relevant for studying the spatially distributed occurrence of surface runoff in natural conditions. They do not allow a comprehensive mapping of areas sensitive to surface runoff at a catchment scale.

A method for surface runoff susceptibility mapping, (called IRIP: French acronym for Intense Pluvial Runoff Index) was proposed by Dehotin and Breil (2011b). It is based on spatial analyses of landscape factors and allows a comprehensive mapping of areas sensitive to surface runoff production, transfer paths and accumulation at a catchment scale, without explicit hydrological modeling. The objective of the experimental study presented in this paper is to assess the relevance of this mapping method, i.e. to verify that runoff occurrence is larger in areas pointed out to be prone to surface runoff by the method. We are therefore interested in getting a spatialized evaluating of runoff occurrence. For this purpose,

we use a distributed network of soil water content measurement sensors and rain gauges stations, with a high temporal resolution to estimate surface runoff occurrence frequency.

The experimental catchment and the observation strategy are presented in section 2, follows by the monitoring protocol for surface runoff occurrence detection and the analysis methods. Section 3 details and discusses field observations. Section 4 synthetizes the experimental results, discusses the limits of the proposed field instrumentation and illustrates its potential for holistic field observations of catchment response.

2. MATERIALS AND METHODS

2.1. Experimental catchment description

The Mercier stream catchment (7 km^2) is located near Lyon city in France (Fig. 1). It is a small rural catchment with low urbanization, covered mainly with forests located upstream and crops located downstream of the catchment. The upstream part of the catchment should not be very sensitive to surface runoff because of the mitigation role of vegetation. Catchment's geology is composed of granite and gneiss with soils characterized by a large spatial variability (SIRA, 2012). The catchment is characterized by permeable soils with permeability values ranging from 0.01 to 0.001 mm h^{-1} (Gonzalez-Sosa et al., 2010). The high soil permeability is expected to lead to a low sensitivity of the catchment to surface runoff by infiltration excess. Upstream of the catchment, soils are very shallow (<0.1m). This catchment is part of a long term Field Observatory (OTHU project)[1]. Collected data were used in several research programs such as the AVuPUR project (Assessing the Vulnerability of PeriUrban Rivers) described in Braud et al. (2010) and Braud et al. (2013). This project also provided a part of the data used in this study, such as a LIDAR digital elevation model (Sarrazin, 2012), a high resolution land use map derived from aerial photos (Jacqueminet et al., 2013), and *in situ* soil hydraulic properties (Gonzalez-Sosa et al., 2010).

[1] Field Observatory for Urban Water Management, http://www.graie.org/othu/

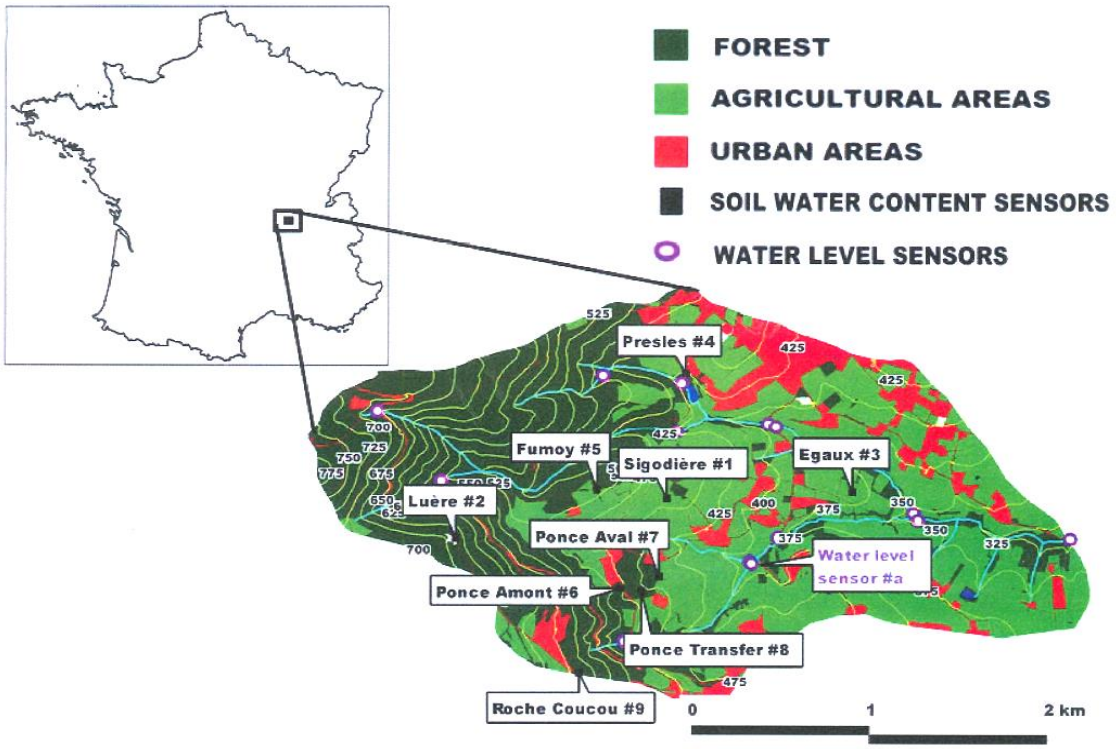

Fig. 1: Location of the Mercier catchment in France and location of the observation sites for soil water content measurements (#1-#9) and locations of water level monitoring (#a) in the river (Sarrazin, 2012)

2.2. Presentation of the IRIP method for surface runoff mapping

The IRIP method is based on a spatial analysis, from upstream to downstream a watershed, of potential occurrence of surface runoff, using landscape factors relevant to describe surface runoff generation, transfer and accumulation (Dehotin and Breil, 2011b). These factors include topographic factors (slope, wetness index, drained area index and break slope), soil parameters (soil thickness, soil permeability and soil erodibility) and land use (urbanized, agricultural or forest areas). The method produces three maps depicting sensitivity of various landscape areas to produce, to transfer or to accumulate surface runoff. Rainfall characteristics are not considered. Thus the method aim is to identify areas that are most likely to produce surface runoff. Areas sensitive to surface runoff production are derived from slope, land use, soil permeability, soil thickness, soil erodibility and topographic wetness index. Each sensitivity map is classified in two classes: sensitive/not sensitive to surface runoff production. Then all the maps are summed up leading to a sensitivity index between 0 (no sensitivity) to 5 (high sensitivity) to surface runoff production. The same principles are applied to derive the two other maps Transfer paths are mapped using topographic analysis which provides slope, break slope, upstream drained area, shape Horton index (Horton, 1945) and linear features such as roads and railways. The latter can divert the flow and induce artificial flow paths, or create water accumulation (roads for instance). An index of upstream surface runoff production is also integrated (transfer path depends on the existence of production areas upstream). Areas sensitive to surface runoff

accumulation are derived from slope, break slope, upstream drained area shape Horton index, upstream surface runoff production index and a topographic wetness index. Evaluating the relevance of these maps requires distributed observations of surface runoff occurrence (yes or no signal). Simple and distributed devices, placed at representative sites are needed for assessing the mapping relevance. Maps generated by the IRIP method on the Mercier catchment are illustrated in Fig. 2. They were used to select the locations of the observation sites (Fig. 1). The latter were chosen to sample different areas sensitive to surface runoff production, transfer and accumulation respectively (see Table 1).

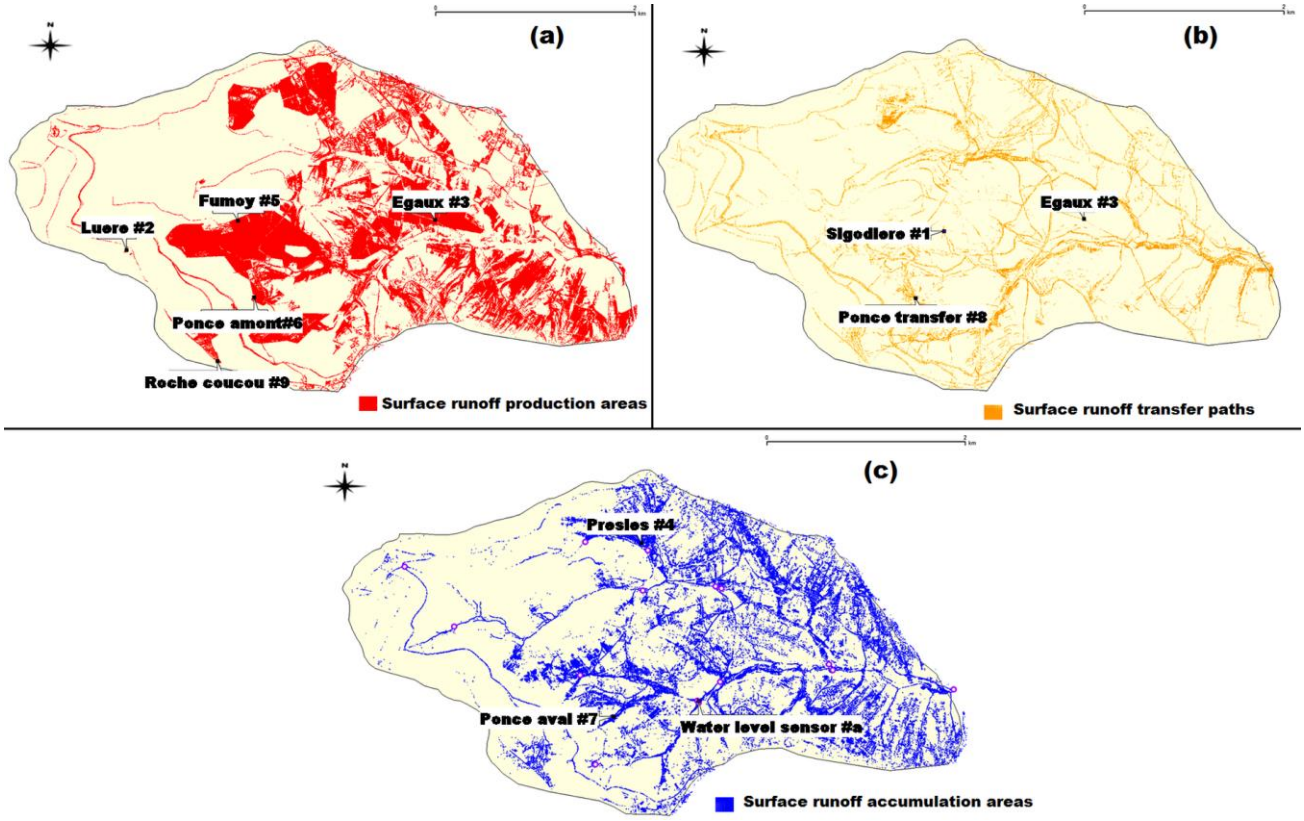

Fig. 2: Surface runoff production (a), transfer (b) and accumulation (c) susceptibility maps in the Mercier catchment showing sensors location

Sites number	stations	Altitude (m)	Location on hillslope	Slope (m/m)	Landuse	Expected susceptibility to runoff	Conductivity ($mm.h^{-1}$)	Saturated water content ($m^3\ m^{-3}$)	Surface runoff frequency (%)
#1	Sigodiere	457	Transfer path	0.14	Crops	Transfer	0.0150	-	-
#2	Luere	667	Upstream	0.23	Forest	Production	0.0088	0.41	5%
#3	Egaux	382	Transfer path	0.08	Crops	Production /Transfer	0.0150	0.47	44%
#4	Presles	426	Downstream	0.1	Pasture	Accumulation	0.0042	0.47	85%
#5	Fumoy	512	Upstream	0.18	Pasture	Production	0.0098	0.43	50%
#6	Ponce Amont	495	Upstream	0.34	Pasture	Production	0.0150	0.54	53%
#7	Ponce Aval	438	Downstream	0.15	Pasture	Accumulation	0.0380	0.46	75%
#8	Ponce Transfert	458	Transfer path	0.17	Pasture	Transfer	0.0150	0.37	47%
#9	Roche coucou	599	Upstream	0.3	Urban	Production	0.0098	0.45	60%

Table 1: Measurement sites description

2.3. Field instrumentation

The observation strategy aims at detecting two runoff mechanisms, using distributed observation devices: surface runoff by infiltration excess and surface runoff caused by saturation of the soil surface horizon. Soil water content time series were recorded continuously in order to detect at each site, potential water ponding at soil surface, for each significant rainfall event. A first set of 20 potential sites was selected from the mapping results. Field constraints limited the number of measurement sites to nine. These constraints are related to field accessibility and authorizations from residents or farmers. A one year (from 09/04/2010 to 08/04/2011) measurement campaign was organized (de Lavenne, 2010) to record surface runoff occurrence and to identify active surface runoff mechanisms. Nine water content sensors (SM100 from Spectrum Technologies Corporation) were installed (9 sites over 7 kilometers) to record continuously soil water content with a 5 to 15 minutes time step (3-5cm below the soil surface). The existing rainfall stations network was extended to 5 rain gauges (almost 1 site per square kilometer). Rain gauges were recorded with a time step of 5 minutes. All electronic devices were connected to small data loggers (WatchDog mini stations from Spectrum technologies) from which data were downloaded each month by an operator (Fig. 3-a).

Measurement sites characteristics are presented in Table 1. Four sites are located upstream the slope (‘*Luere’-#2*, *Fumoy’-#5*, ‘*Ponce Amont’-#6* and ‘*Rochecoucou’-#9*) and two sites are located downstream the slope (‘*Presles’-#4* and *‘Ponce Aval’-#7*). The ‘*Egaux’-#2, ‘Sigodiere’-#1* and ‘*Ponce Transfert’-#8* sites are located within surface runoff transfer paths. At the ‘*Ponce Amont’-#6* (site located upstream the slope), two sensors were installed at the same location: one at 3-5 cm from the top soil and another one at the bedrock, located 10 cm below the soil surface. It allows analyzing subsurface flow occurrence. Three measurement sites (‘*Ponce Amont’-#6, ‘Ponce Transfert’-#8 and ‘Ponce Aval’-#7*) are located on the same hillslope, from upstream to downstream in order to observe event surface water dynamics in a hillslope.

Continuous records were complemented with rainfall post-event field observations. They are based on a network of 24 water traps designed and installed close to the monitoring devices, with 3 water traps per site on average. A water traps consists in a PVC tubes with 5 cm in diameter, perforated in its top part and closed at each extremity to avoid direct rainfall input on top and to create storage capacity at the bottom. They were installed in the first 5cm depth soil layer in the perforated zone, closed at the top (Fig. 3b). This device is expected to intercept surface runoff generated during a rainfall event. Water traps content were emptied after each significant rainfall event in order to be sure that the water they contain was associated with the most recent rainfall event. These observations were used to confirm occurrence of surface runoff both by saturation of the first soil horizon and by infiltration excess highlighted by the continuous sensors records.

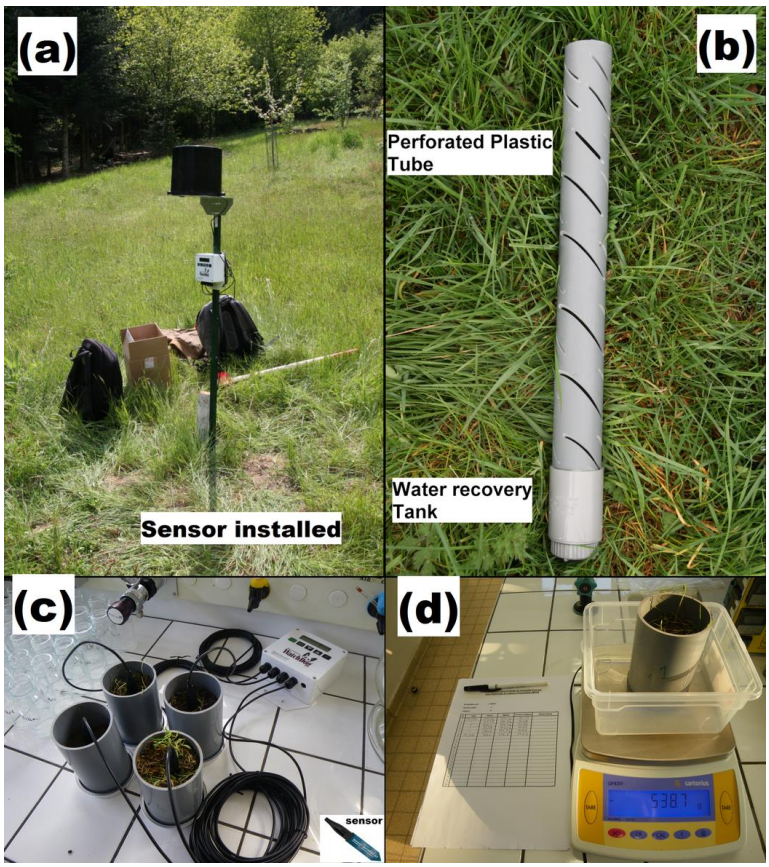

Fig. 3: Photos of the soil water content measurement sensor (a), water traps (b) installed in the catchment and soil moisture sensor calibration in the laboratory with in-situ soil (c-d)

2.4. Soil water content sensors calibration

A relationship relating sensors readings to soil water content is provided by the constructor. We performed laboratory measurements in order to verify these relationships. We used gravimetric soil samples taken in the field at each measurement site (Fig. 3c, 3d). Each sensor was calibrated for each site with the corresponding in-situ soil sample. A known volume of soil sample taken from the field was saturated, drained and dried in an oven in the laboratory. Samples were saturated from the bottom (as long as needed to reach full saturation of soil sample) and a first value of soil water content was measured by the sensor. Soil samples were then left dry by gravity and their saturated soil mass computed, knowing the container weight. Soil samples were dried and their weights were measured periodically as well as the corresponding sensor reading. When the soil sample got dry (after one week), the soil was oven-dried at 105° during 48 hours. The oven dry weight was measured and the sensor value was read. Volumetric water content at each site was calculated using the following equation:

$$H_v = 100 \times \left[\frac{(m_i - m_{dry})}{(\rho_w \times V_{tot})} \right] \quad (1)$$

where H_v is the volumetric water content ($m^3\ m^{-3}$), m_i the mass of soil at a given water content during dry down, m_{dry} (kg) the oven-dry soil mass, V_{tot} (m^3) the total soil volume and ρ_w the water volumetric

mass (kg m^{-3}). These measurements confirmed the constructor relationships which was further used in the study.

Saturated soil water content value was used to follow-up the first soil horizons saturation during each rainfall event. From this analysis the effective saturated soil water content in the Mercier catchment is variable and ranges from 37 to 54% (Table 1) according to soil samples from measurement sites.

2.5. Data processing

The method used to process the recorded data is presented in Fig. 4. It allows identification of surface runoff occurrence and its type (Hortonian or saturation of the soil surface horizon) for each observation which is defined as a couple (rainfall event and measurement site).

Surface runoff by infiltration-excess is detected by comparing soil infiltration capacity time series and rainfall intensity time series. Infiltration capacity time series are computed from field records of soil initial water content (recorded before each rainfall event) and field measures of soil surface hydraulic conductivity. The mechanism of infiltration-excess is illustrated in Fig. 5a. During a rainfall event, soil infiltration capacity (in mm h^{-1}) decreases quickly to reach a near constant infiltration value when the soil is saturated, corresponding to the saturated hydraulic conductivity. If rainfall intensity (also in mm h^{-1}) exceeds the infiltration capacity, surface runoff can occur. Infiltration capacity is computed using the Smith and Parlange (1978) equation:

$$f = K_s \frac{\exp(F/B)}{[\exp(F/B)-1]} \quad (2)$$

where f is the infiltration capacity, function of time, K_s is the saturated hydraulic conductivity, F is the cumulative infiltration, B is a parameter related to the saturation deficit :

$$B = G(\theta_s - \theta_i) \quad (3)$$

G is the net effective capillarity, G was estimated from Smith et al (2002). It is a function of soil texture. θ_s is the saturated soil moisture and θ_i is the initial water content at the beginning of the rainfall event. *In situ* soil water content reading from the sensors were used to specify θ_i. The soil saturated hydraulic conductivity used for computation is taken from in-situ values, derived from positive head and tension disk infiltrometer infiltration tests presented in Gonzalez-Sosa et al. (2010). Values are provided in Table 1.

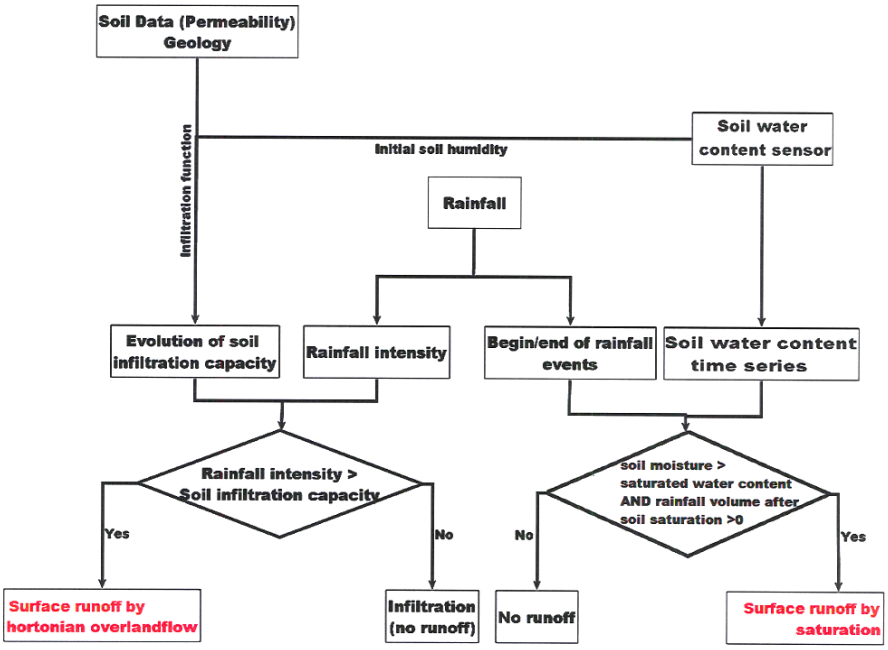

Fig. 4: Overview of the data processing method for the detection and identification of the surface runoff type

The second surface runoff mechanism detected using the collected data is surface runoff by saturation of the soil surface horizon. Indeed, in our catchment, characterized with shallow soils and relatively high values of saturated hydraulic conductivity (see section 2.1), a decrease of hydraulic conductivity with depth was observed using in situ data. This can favor the apparition of perched water tables, leading to the saturation of the top soil horizon, but not of the full profile. In agricultural areas, such hydraulic conductivity contrasts can be induced by ploughing. This type of runoff was detected by comparing soil water content time series with the saturated values provided in Table 1. During each rainfall event, soil surface saturation state is checked using the continuous record of soil water content. When rainfall continues after soil saturation, it is assumed that water ponding has occurred and runoff on saturated surface can start. A similar procedure was used by Schmocker-Fackel (2007) for identifying surface runoff process using a set of rainfall and piezometers data in a small catchment. Surface runoff by saturation of the soil surface horizon is illustrated in Fig. 5b. During a rainfall event, soil water content rises and the soil can become saturated. We assume that it happens when soil water content time series reach a plateau and remain almost constant, with a value close to the laboratory soil saturated water content. When this constant value is reached, we assume that the first soil horizon is saturated and additional rainfall is generating surface runoff until the rain stops.

All the recorded data were used to compute the occurrence of surface runoff. The role of rainfall event characteristics on surface runoff mechanisms and relationships between observed surface runoff frequency and several landscape factors on surface runoff occurrence were also analyzed. A single dimensional approach and a multi-dimensional analysis are performed. The multi-dimensional analysis is based on Factorial Analysis of Mixed Data (FAMD) proposed by Pagès (Pagès, 2004), using the

FactoMineR package (Lê et al., 2008). In the analysis we considered the observations as "individuals" and the following variables: six quantitative variables: event cumulated rainfall, event maximum rainfall intensity, event rainfall duration, saturated hydraulic conductivity, soil depth and initial soil moisture and two qualitative variables with two modalities (yes/no): occurrence of saturation runoff, occurrence of hortonian runoff. Runoff occurrence was considered as a supplementary variable as it is redundant with the two others (runoff occurrence is yes if either saturation or hortonian runoff occurrence is yes). The FAMD function of the R package was used for this purpose. Hierarchical Clustering of Principal Components (HCPC function of the package) was performed.

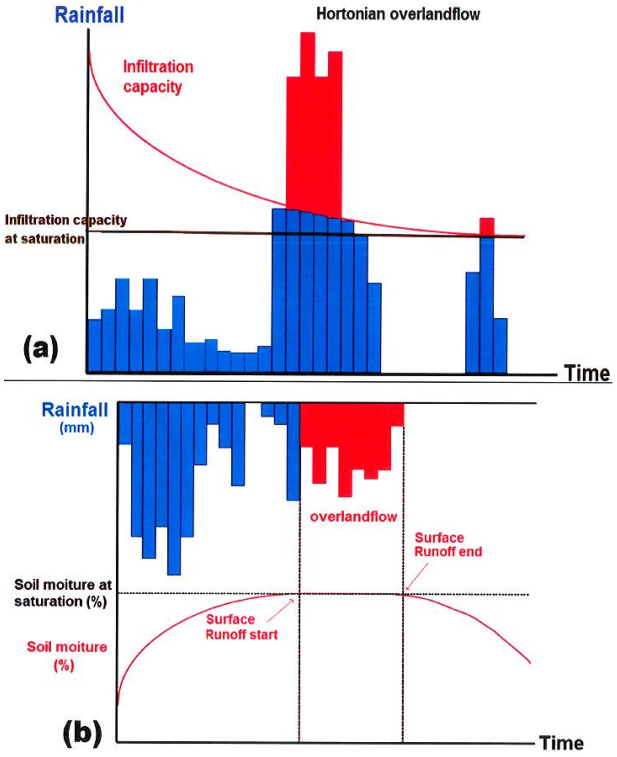

Fig. 5: Illustration of the detection of surface runoff: (a) by the Hortonian overland flow (comparing rainfall intensity and infiltration capacity) and (b) by saturation excess (checking rainfall event after soil saturation)

3. RESULTS

3.1. Rainfall events characteristics

A total of 15 significant rainfall events were analyzed. Combined with the 9 measurement sites, it leads to a total of 183 observations. Rainfall events are considered as significant when rainfall accumulation is larger than 10 mm or if a maximum intensity larger than ten millimeter per hour over 5 minutes (*10 mm* h^{-1}) is reached. These threshold values were chosen after analyzing all recorded data and considering a rainfall amount that induced significant changes of soil water content, or rainfall events with a maximum intensity larger than the minimum observed saturated hydraulic conductivity.

Recorded rainfall events lasted from a few minutes to a few days. As shown in Fig. 6, the rainfall intensity and accumulation were highly variable. The highest value of rainfall intensity is *132 mm* h^{-1}

over 5 minutes, and the largest value of rainfall accumulation is about *139 mm* in one day. Against all expectations (given the small catchment size), a high spatial variability of the rainfall accumulation between the rainfall gauges in the catchment is observed. The standard deviation of the annual rainfall accumulation between the five rain gauges is about *114 mm*. As reference, *82 mm* is the average standard deviation of inter-annual rainfall amounts for the catchment from existing monitored rain gauges stations (Braud et al. 2013).

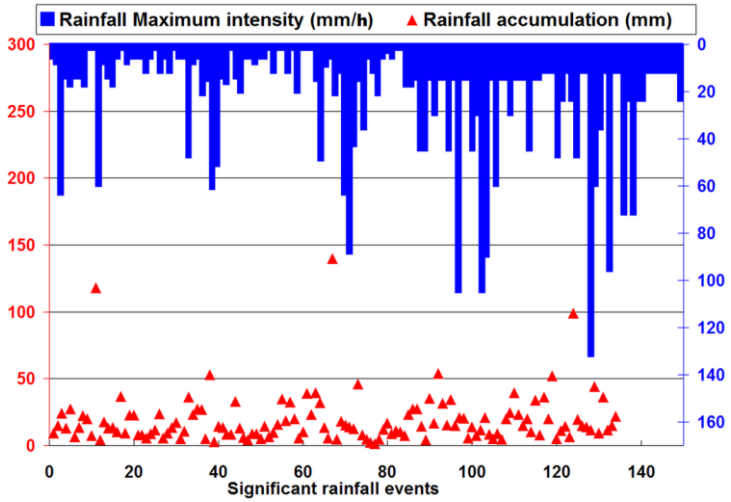

Fig. 6: Distribution of rainfall accumulation and maximum intensity for the observed significant rainfall events

We also observed, for various rainfall events, a significant spatial variability of the maximum intensity between rainfall gauges. For each rain gauge, rain accumulation and maximum rainfall intensity are reported in Table 2. The total rain accumulation over the observation period is *587.6 mm* and the mean of the maximum rainfall intensity for the different stations is about *90 mm* h^{-1}over 5 minutes. The mean temporal interval between two rainfall events on the different sites ranges from 6 days to 10 days. The minimum time interval observed is about 12 hours. Previous rainfall may influence initial soil moisture and later on soil initial infiltration capacity but given the relatively high infiltration capacity of the soils (see section 2.1) and the quick drainage of the surface soil layer (see section 3.4.3), we consider the hypothesis of independence of rainfall events as reasonable. Moreover, other hydrological processes, such as subsurface lateral flow, may also influence the initial soil moisture.

Location number	Rain station	Rain accumulation during the observation period (mm)	Max Intensity (mm h^{-1})
#1	Sigodiere	587,7	88,8
#2	Luere	584,3	63,6
#3	Egaux	569,5	105,0
#4	Presles	437,9	61,2
#9	Rochecoucou	758,6	132,0
	Mean	**587,6**	**90,1**
	Standard dev	**114,0**	**29,7**

Table 2: Observed rainfall characteristics by rainfall gauge on the Mercier catchment

3.2. Surface runoff occurrence frequency in the Mercier Catchment

All rainfall events were analyzed following the strategy depicted in Fig. 4 and 5. Surface runoff occurrence was checked by analyzing field data. Fig. 7 illustrates an observation data from the '*Ponce Amont*'-#6 site. In this example, two surface runoff mechanisms are detected.

In the upper part of Fig. 7, the horizontal red line is the value of saturated soil water content. The grey band surrounding the red line represents the uncertainty range of sensor records, as provided by the constructor (around 2%). The blue dots curve is the time series of soil surface water content during the rainfall event. While soil water content remains inside the grey band, the top soil is considered as saturated. Therefore, any additional rainfall will induce water ponding and surface runoff by saturation of the soil surface horizon. The orange line in Fig. 7 represents the soil saturated hydraulic conductivity. Infiltration capacity during the rainfall event (green line in Fig. 7) is calculated using Eq. 2. Infiltration capacity is always higher than soil saturated hydraulic conductivity. Until rainfall intensity remains higher than infiltration capacity, surface runoff by infiltration excess can occur.

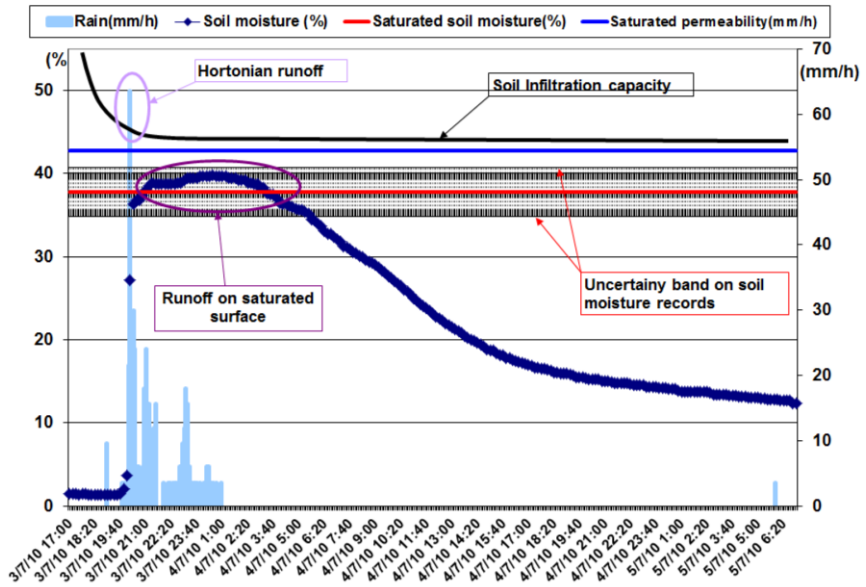

Fig. 7: Illustration of surface runoff detection from recorded data on the 'Ponce Amont'-#6 station. Surface runoff by Hortonian overland flow is detected by comparing rainfall intensity and infiltration capacity. Surface runoff on a saturated surface occurs when rainfall continue after soil saturation

Several rainfall events and measurement sites were chosen to illustrate representative cases of surface runoff identification (Fig. 8). These graphs are similar to those of Fig. 7. At the '*Ponce Amont*'-#6 site (Fig. 8a), only surface runoff on saturated surface (see water content time series) is detected. Hortonian runoff is identified in Fig. 8b at the '*Luère*'-#2 site (rainfall intensity curve greater than the infiltration capacity). Both mechanisms leading to surface runoff are observed at the '*Egaux*'-#3 site (Fig. 8c) whereas no surface runoff occurs at the '*Ponce Tranfert*'-#8 site (Fig. 8d).

In practice, it was not always easy to make a distinction between different runoff mechanisms, especially when the two processes occur at the same time. In these cases, high rainfall intensity induces saturation of the first soil horizon. Even if infiltration continues, water ponding can occur at the soil surface. In such cases it is considered that the two surface runoff mechanisms probably occur. However, this situation was rarely observed (four times on the whole data set). The confirmation of detected surface runoff was performed using the water traps devices presented in Figure 3b. Ten of the fifteen significant rainfall events were followed by field observations. Analyzing field observation sheets, a total of 160 observations were followed by a field observation.

This analysis is performed for each site and for each significant rainfall event, using the 183 observations. Surface runoff frequency is then defined as the number of detected surface runoff divided by the number of observations. In the Mercier catchment *34%* of *183* observations generate surface runoff. Saturation excess represents *70%* of the detected surface runoff events. It is thus the most frequent mechanism observed in the Mercier catchment. Fig. 9 and Table 1 present a synthesis of surface runoff frequency for the different runoff mechanisms, at each observation site. Fig. 9 confirms that surface runoff by saturation of the soil surface horizon is the most frequent surface runoff process at sites located downstream the slope (#4 and #7). Two sites located upstream the slope (#2 and #5) are more sensitive to surface runoff by infiltration excess.

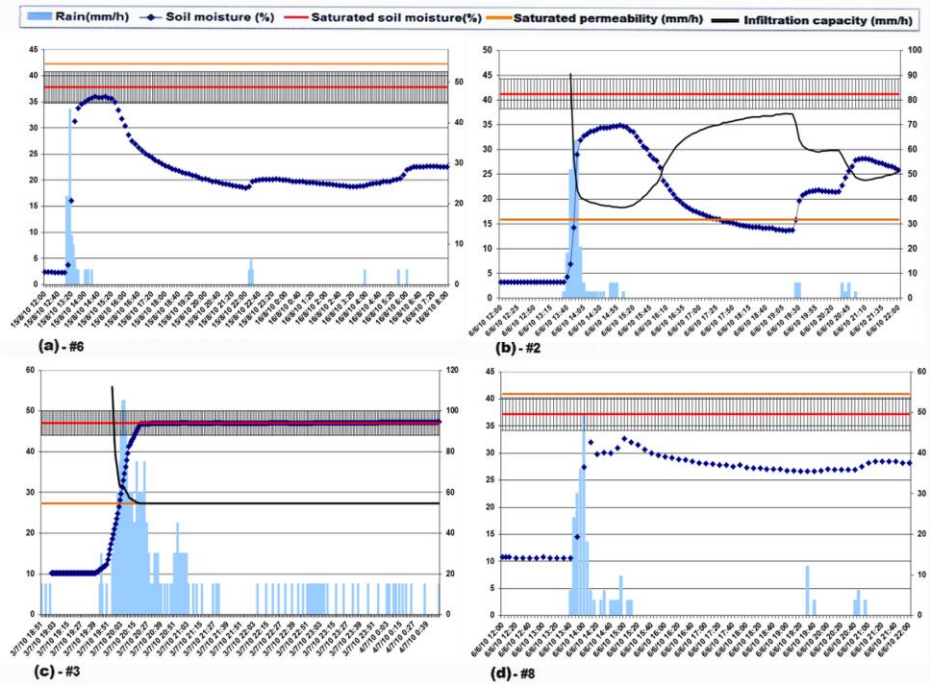

Fig. 8: Some examples of runoff detection graphs at 'Ponce Amont'-#6 (a), 'Luere'-#2 (b), 'Egaux'-#3 (c) and 'Ponce Transfert'-#8 (d) stations

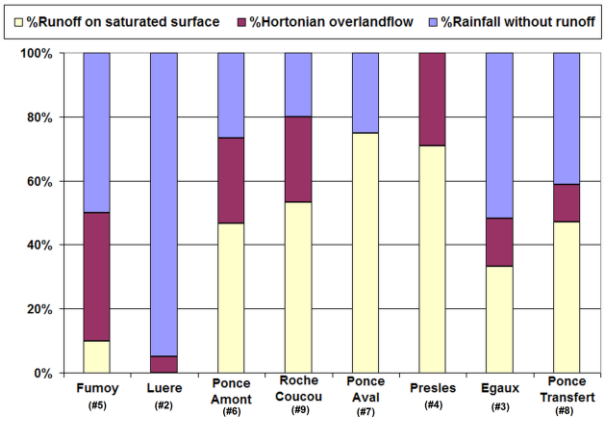

Fig. 9: Runoff detection rate for different kinds of surface runoff for all the runoff events at each observation site

3.3. Role of rainfall accumulation and intensity on runoff occurrence

Relationships between surface runoff frequency and two rainfall characteristics are examined: rainfall accumulation and maximum rainfall intensity over 5 minutes. All the *183* observations are grouped into 4 classes of rainfall intensity. Similarly, the observations are also grouped into 3 classes of rain amount per event. Surface runoff frequency is computed for each class of rainfall maximum intensity (Fig. 10a) and of rainfall accumulation (Fig. 10b).

Fig. 10a shows that the frequency of surface runoff by infiltration excess increases when rainfall intensity increases. We also observe that for rainfall maximum intensity less than 15 mm h^{-1}, no surface runoff by infiltration excess is detected while all rainfall events with a maximum intensity higher than 60 mm h^{-1} induce surface runoff. In this case, surface runoff by infiltration excess is the most frequent mechanism. The frequency of surface runoff on saturated surfaces increases with rain accumulation (Fig. 10b). These results are consistent with our expectations and with results from other authors (e.g. Dunne et al., (1991); Assouline and Ben-Hur, (2006)). Another interesting result shown in Fig. 10 is that low rain accumulation or low maximum rainfall intensity can also induce surface runoff. It confirms that despite the large impact of rainfall on runoff generation, neither rain intensity nor amount of rainfall accumulation is able to fully explain surface runoff occurrence.

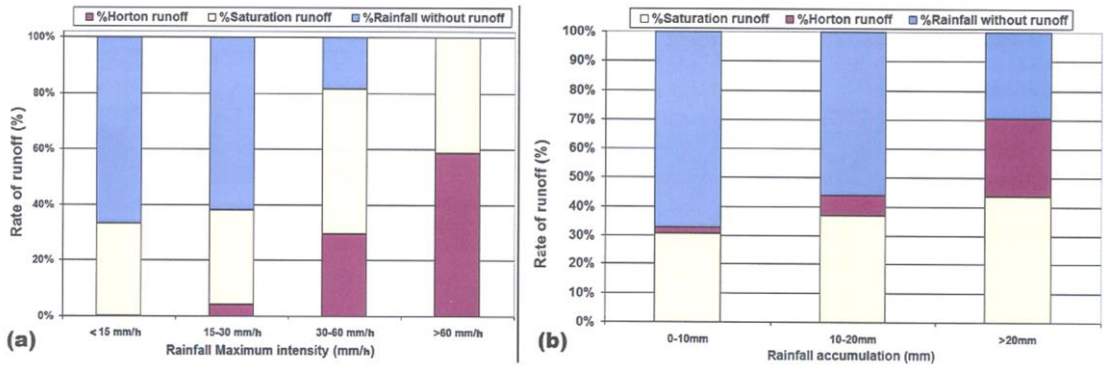

Fig. 10: Observed relationship between surface runoff frequency and (a) maximum intensity and (b) rainfall accumulation

3.4. Role of several landscape factors on runoff generation

The main hypothesis of the IRIP mapping method is that surface runoff occurrence is explained by a set of favorable landscape factors as depicted in Dunne et al. (1975). Measurement sites have different characteristics (e.g. slope, soil hydraulic properties and land use etc.) as presented in the section 'Materials and methods'. The goal of the present section is to use our experimental data to describe and analyze relationships between surface runoff frequency and some landscape factors, namely soil hydraulic conductivity, soil thickness and soil initial water content. The impact of other parameters such as slope, soil erodibility and topographic index is not analyzed due to the lack of spatial variability of those parameters amongst measurement sites.

3.4.1. Soil saturated hydraulic conductivity

In order to assess the role of soil hydraulic conductivity on surface runoff, observations are grouped into 5 classes according to their soil saturated hydraulic conductivity. These classes (Table 1) broadly represent silty and sandy soils. Each class includes one or more measurement sites. About 36 observations are analyzed per class (Table 3). Surface runoff frequency is computed as the ratio between the total number of observations in each hydraulic conductivity class and the total number of observations in the class. Fig. 11a presents the surface runoff frequency for different classes of hydraulic conductivity. In the radar graph (Fig. 11b), each axis represents classes of hydraulic conductivity. Two kinds of behaviors are observed. The most impervious soil (silt) is sensitive to surface runoff by Hortonian mechanism whereas sites with high hydraulic conductivity are mainly sensitive to surface runoff by saturation of the soil surface horizon. These results confirm the role of soil hydraulic conductivity on surface runoff generation, as also pointed out by several authors (Blanco-Canqui et al., 2002; Dunne and Black, 1970). The class with conductivity value of 0.0088 $mm.s^{-1}$ (#2) is located on forest. Only one surface runoff occurrence was identified, despite the value of soil permeability. This situation is probably due to the attenuation role of vegetation on surface runoff generation.

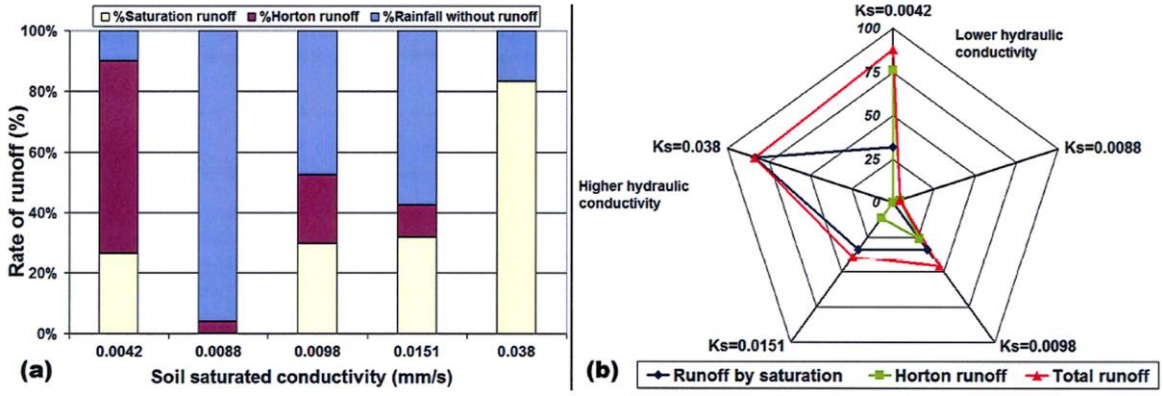

Fig. 11: Relationship between soil hydraulic conductivity and surface runoff frequency plotted as (a) an histogram and (b) a radar graph

Hydraulic conductivity classes	Number of observed rainfall events
0.0042	25
0.0088	25
0.0098	50
0.0151	71
0.038	12
Mean	**36.6**

Table 3: Rainfall events for each class of hydraulic conductivity

3.4.2. Soil thickness

The range of soil thickness at measurement sites is limited to only two categories: soils with thickness lower than 15 centimeters and soils with thickness larger than one meter. Measurement sites were grouped in two classes: site with soil thickness lower or larger than one meter. As in the previous section, each class includes several measurement sites (Table 4). Surface runoff frequency is the sum of total occurrences of surface runoff of the class, divided by total number of analyzed observations in the class. Fig. 12 shows surface runoff frequency for different soil thickness classes. Overall more surface runoff occurs on deeper soils against all expectations, as it is generally assumed that soils with low thickness are more sensitive to surface runoff than soils with large thickness. However, our result is influenced by sites location. Sites with a high value of soil thickness are located downstream the slopes, in water accumulation areas whereas sites with a small soil thickness are located upstream the slope where soils are well drained and shallower. These results cannot be extended to the whole catchment because the set of measurement sites is not representative of the catchment soils thickness distribution.

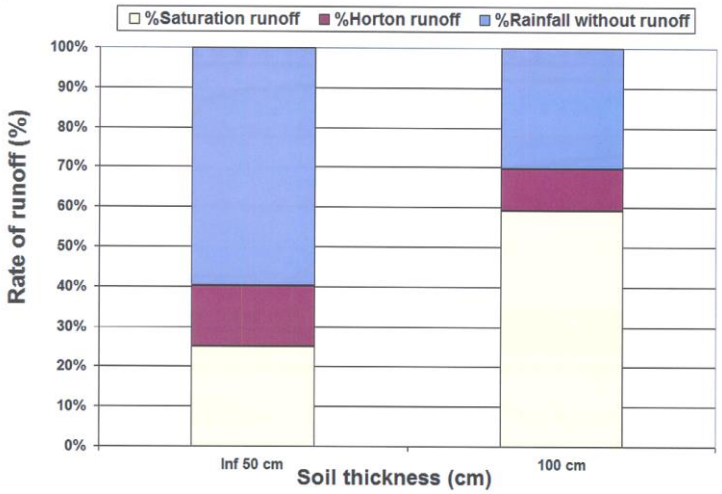

Fig. 12: Relationship between soil thickness and surface runoff occurrence

Soil thickness classes	Number of observed rainfall events
<=100 cm	33
> 100 cm	60
Mean	**46.5**

Table 4: Rainfall events for each class of soil thickness

One of the most common assumptions about the role of soil thickness is to assume soil saturation from the bottom of shallow soil layers. After filling the porosity within the soil matrix, it would result in surface runoff on saturated surface. This surface runoff mechanism occurrence was analyzed in the experimental catchment. Fig. 13 shows the evolution of soil water content at the '*Ponce Amont'-#6* site, near the soil surface (blue dots curve) and near the bedrock 10 cm below the topsoil (green curve). Surface runoff on saturated surface is detected. However, close to the bedrock, no saturation is observed. Soil water content value is lower than 10% whereas the value at saturation is about 35%. In this case, no surface runoff by saturation excess, due to the whole soil profile saturation from the bedrock is detected.

In conclusion, the role of soil thickness could not be clearly demonstrated in the context of this field experimentation. However impacts of soil thickness on runoff generation was shown by authors such as Sharpley (1985), Power et al (1980), Peters et al, (1995) or more recently Rahimy (2012). Sampling a larger soil thickness range would have been necessary to more clearly demonstrate the role of soil thickness. As shown by Graham et al (2010), bedrock permeability may also play an important role on subsurface flow, that can impact the occurrence of surface runoff. The role of bedrock permeability on above bedrock soil water content evolution is not analyzed in this study.

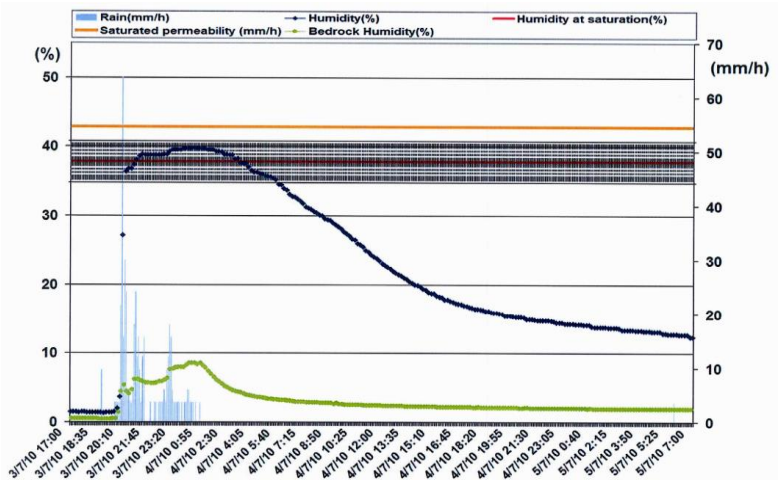

Fig. 13: Time series of soil water content during a rainfall event near the soil surface (-3cm) and near the bedrock (-10cm) at Ponce Amont station #6

3.4.3. Soil initial water content

Initial soil water content is one of the most discussed factors in the literature regarding its role in initiating surface runoff. This role is here analyzed using *in-situ* values measured for each rainfall event, few minutes before the beginning of the event. Initial soil water content for the *183* observations were grouped into five (5) classes of initial water content (0-10%; 10-30%; 30-*50%; 50-75%; 75-100%*). As in the previous sections, each class includes one or more measurement sites. In this case, each site may be included in different classes, as initial water content may be different from one rainfall event to another. Surface runoff frequency is the sum of total occurrences of surface runoff of

the class divided by the total number of observations in the class. Table 5 presents the number of observations analyzed for each class. Fig. 14 presents surface runoff frequency as function of soil initial water content classes. In the radar graph, each axis represents a different initial water content class. Fig. 14 shows that more surface runoff occurs for high soil initial water content. In Fig. 14a, two trends are observed. Limited surface runoff occurs at very low initial water content (0-10%). High values of initial water content are linked to significant surface runoff frequency. These results confirm the hypothesis of low infiltration on wet or saturated soils, in the IRIP surface runoff mapping. It is also consistent with usual results about the role of soil initial water content on surface runoff and erosion (Castillo et al., 2003; Govers and Loch, 1993; Hino et al., 1988; Huang et al., 2002; Le Bissonnais et al., 1995; Truman et al.). In the radar graph of Fig. 14b, surface runoff occurs for very low initial soil water content, mainly by Hortonian mechanism. This result may be explained by water repellency of dry soils that makes these soils sensitive to surface runoff (Badoux et al., 2006; Dekker and Ritsema, 2000).

Soil initial water content classes	Number of observed rainfall events
0-10 %	33
10-30 %	33
30-50 %	31
50-75 %	33
75-100%	53
Mean	**36.6**

Table 5: Rainfall events for each class of soil initial water content

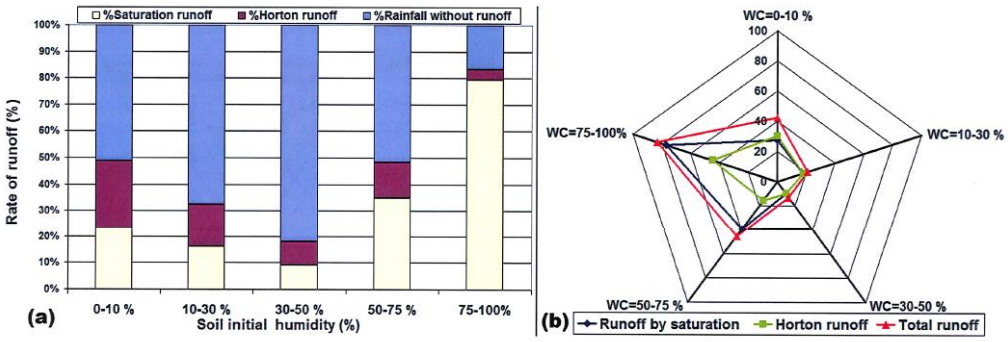

Fig. 14: Relationship between soil initial water content (WC) and surface runoff occurrence plotted as (a) an histogram (a) and (b) a radar graph

Effects of soil initial water content depend on the sites location within the catchment (upstream or downstream the slope). Fig. 15a shows that observation sites located downstream are more sensitive to surface runoff by saturation excess and sites located upstream are more sensitive to surface runoff by infiltration excess. Axes of Fig. 15a represent surface runoff frequency at observation sites. Time series of soil water content (Fig. 15b) show different hydric regime at observation sites located from upstream to downstream the same hillslope. Sites located upstream are quickly drained after rainfall events contrarily to those located downstream the hillslope. Sites located upstream seem less influenced by soil initial water content (Fig. 15a). This observation suggests that the role of initial soil

water content on surface runoff generation must be taken into account mainly in areas located downstream the slope as depicted in Huang et al (2002).

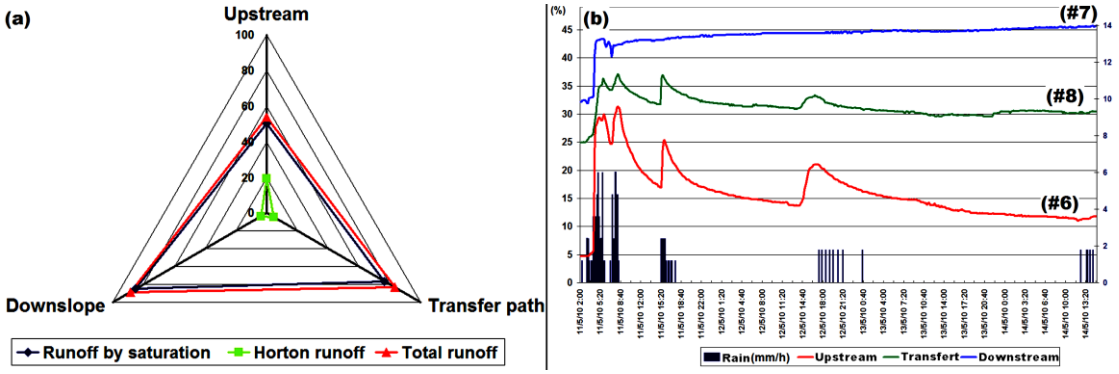

Fig. 15: Relationship between initial soil water content and surface runoff frequency according to the site location (a) and soil water content evolution during a rainfall event at different sites (b) upstream site (#6), transfer path site (#8) and downstream site (#7)

3.5. Single and multi-dimensional analysis of the data set

Fig. 16 summarizes the relative weight of different factors on surface runoff frequency using a single dimensional analysis. In this analysis the effect of each factor on surface runoff is independent from the others. Each axis represents surface runoff frequency for each landscape factor. It is computed, considering all measurement sites and all analyzed rainfall events. Surface runoff frequency at observation sites with the following characteristics are reported on the same graph: high initial water content, low soil permeability, low soil thickness, high rainfall intensity and high rainfall accumulation. Not surprisingly, high rainfall intensity is the main recurrent factor explaining surface runoff frequency. It is followed by low soil permeability, and soil high initial soil water content and high rain accumulation.

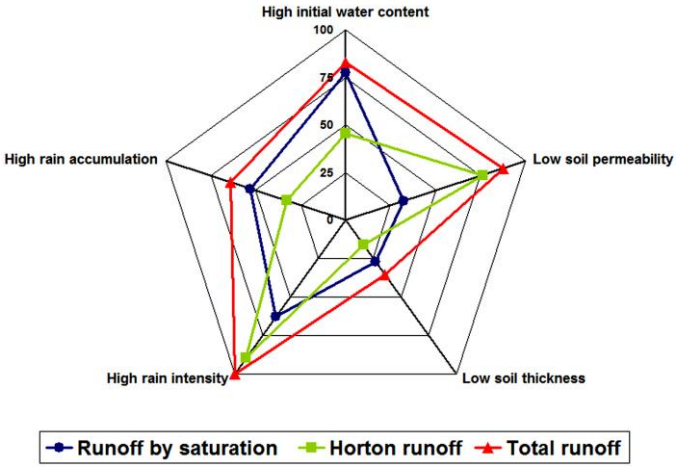

Fig. 16: Relative influence of high initial water content, low soil permeability, low soil thickness, high rainfall intensity and high rainfall accumulation on surface runoff frequency

As explained in section 2.5, we performed a multi-dimensional analysis using the Factorial Analysis of Mixed Data of the data set. It allows analyzing quantitative and qualitative variables at the same time. Quantitative variables are related to Soil Permeability, Soil Thickness, Rain Accumulation, Initial Soil

Moisture, Rain Max Intensity and Rain Duration. Qualitative variables are related to occurrence of hortonian surface runoff (Horton_Run), surface runoff by saturation of soil horizon (Sat_Run) the occurrence of surface runoff whatever the cause (Tot_Run). We analyze the relationships between predisposing factors and the different kinds of surface runoff. Fig 17 and Table 6 summarize the main results of the multi-dimensional analysis. Three dimensions explained 66.5% of the total variance. Thus a good relationship exists between variables. As shown in the correlation circles in Fig 17a, b, c and Table 6, soil thickness and initial soil moisture are highly linked to the first dimension. Soil permeability is linked to dimension 2 and rainfall maximum intensity to dimension 3. Rain accumulation is linked to dimension 1 and 2. Rain duration is not linked to any dimension. The hortonian surface runoff occurrence and the surface runoff by soil surface horizon saturation occurrence are linked to dimension 1 (Fig 17 d, e, f). Fig. 17 g, h, i show the result of Hierarchical Clustering on Principal Components. Cluster 1 includes 'no surface runoff' and is characterized by low initial soil moisture, low soil thickness, low rainfall intensity and low rain accumulation. This result is consistent with our expectation. Cluster 2 is composed of individual with surface runoff by soil surface saturation (90% of members), hortonian surface runoff (51% of members), no surface hortonian runoff (49% of members), high initial soil moisture, high soil thickness, low rainfall intensity and low permeability. Cluster 3 includes individuals with hortonian surface runoff (89% of members), surface runoff be surface saturation (63% of members), no saturation (40% of members), high rainfall intensity, high rain accumulation, low rain duration, low initial soil moisture. At last cluster 4 includes individuals with surface runoff by surface saturation (84% of members), no hortonian surface runoff, high permeability, high soil thickness, high initial soil moisture. The relationship between surface runoff occurrence and type are not as clear as in the single dimension analysis. The results analysis allows relating observations with surface runoff by saturation with high initial soil moisture. More hortonian runoff is observed on sites with low permeability and high rainfall intensities (Clusters 2 and 4). More observations in more contrasting contexts are needed to take a better part of the multi-dimensional analysis.

Variables	**Correlation**			**Cos2**		
	Dim1	**Dim2**	**Dim3**	**Dim1**	**Dim2**	**Dim3**
	0.24	-0.53	0.56	0.06	0.29	0.32
Rain_Max_Int	0.49	-0.70	0.13	0.24	0.49	0.02
Soil_Perm	0.12	0.25	0.77	0.01	0.06	0.60
Soil_Thick	0.65	0.50	0.09	0.42	0.25	0.01
Init_Soil_Mois	0.62	0.61	-0.15	0.39	0.37	0.02
Rain_Duration	-0.32	0.29	0.29	0.10	0.08	0.09
Sat_Run	0.82	0.10	0.14	0.44	0.02	0.00
Hort_Run	0.70	0.37	0.40	0.44	0.00	0.00
Tot_Runoff				0.52	0.00	0.00

Table 6: Results of factorial analysis of mixed

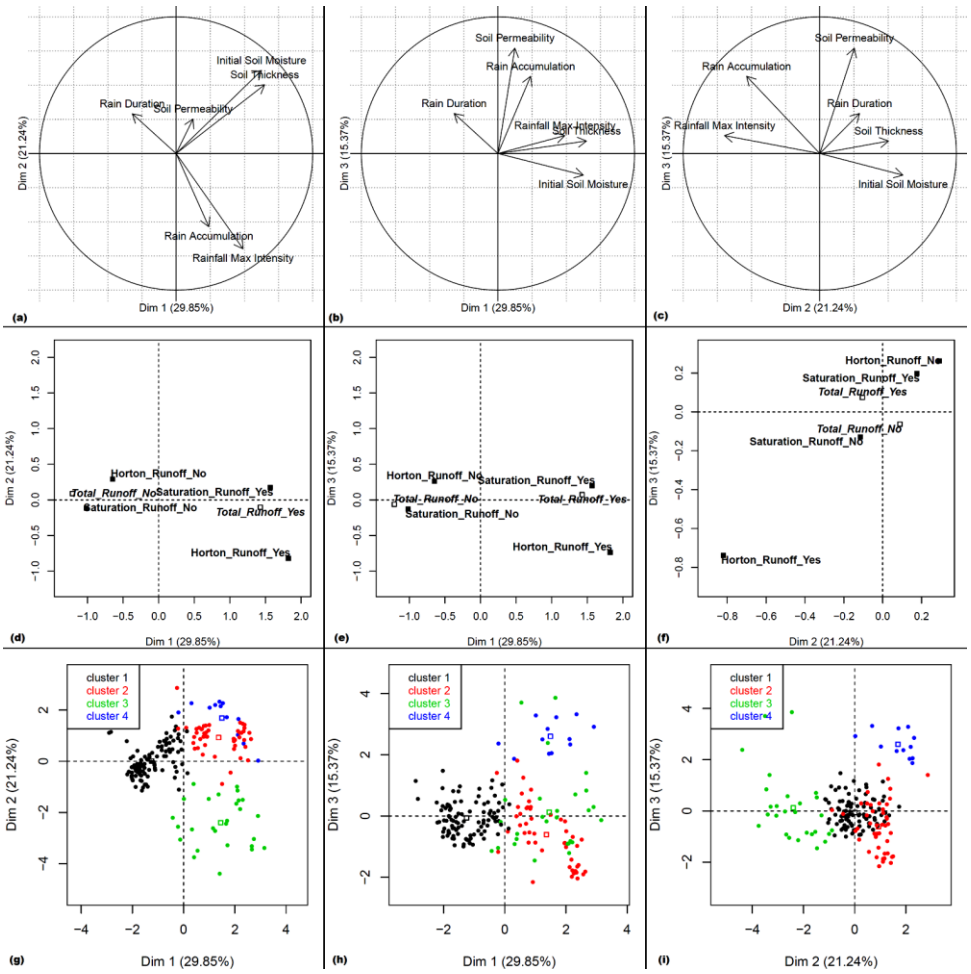

Fig. 17: Results of factorial analysis of mixed data: (a,b,c) Result of correlation circles; (d,e,f) Result of group representation and (g,h,i) Result of Hierarchical Clustering on Principal Components.

3.6. Consistency between observations and surface runoff susceptibility mapping in observation catchment

In the previous sections different assumptions about the role of some landscape factors on runoff occurrence was analyzed in order to evaluate consistency of surface runoff mapping with observations. Generally, sites with high surface runoff frequency are identified as surface runoff accumulation or production areas in the surface runoff susceptibility maps. These results are consistent with our expectations.

Fig.18 and Table 1 presents a comparison of runoff occurrence frequency as compared to the runoff risk mapping results. Overall, sites where surface runoff production or accumulation was predicted (see Table 1 for details) are those where larger surface runoff frequencies were observed.

Results presented in this paper are difficult to generalize to all kinds of catchments. This generalization requires more experimentation in much contrasted catchments and denser observation network.

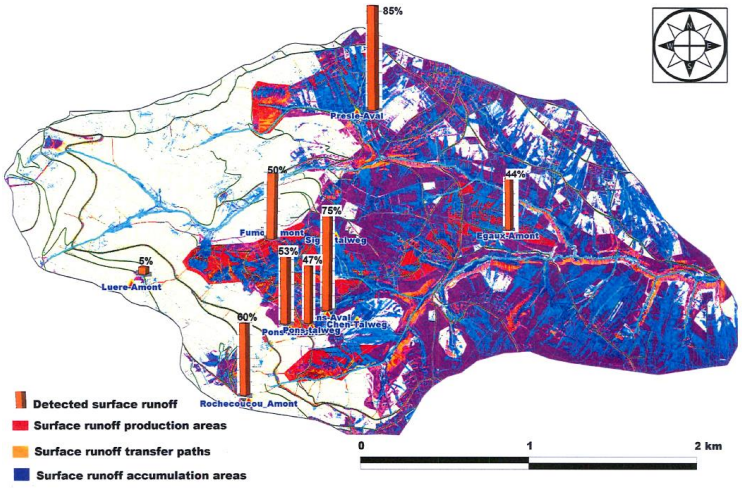

Fig. 18: Surface runoff transfer and accumulation susceptibility map with observed surface runoff occurrence on the Mercier catchment.

4. CONCLUSIONS AND PERSPECTIVES

The presented observation method was used to detect surface runoff in several sites in a small catchment. The presented method consists in distributed observations of surface soil water content in order to identify the occurrence of surface runoff. The presented distributed observation method allows the monitoring of fast and short-lived surface runoff processes at a small spatial and temporal resolution. It also allows highlighting the relationship between surface runoff and different factors usually integrated in surface runoff risk mapping. This link is seldom observed in natural conditions. This method allows detecting both surfaces runoff by Hortonian and surfaces runoff by the saturation of first soil horizons. The saturation from below usually called saturation-excess near the river bank was not addressed in this study since no observation device was setup near river. Analyzed landscape factors are soil depth, soil initial water content, soil permeability, rainfall intensity and cumulative rainfall amount. Two kinds of analysis were performed: single dimensional approach and multidimensional analysis. Other factors such as slope, topographic index or soil erodibility are not studied because their variability among the measurement sites was not sufficient. More observations in more contrasted contexts may allow exhaustive analysis of the role of all landscape factors impacting surface runoff generation.

Compared with usual field measurements of surface runoff, the presented method allows installation of a sensors network, distributed in space, for surface runoff spatial distribution identification and analysis. It also permits to overcome rainfall simulation devices (heavy and expensive) and to analyze directly real rainfall events impact on surface runoff. Contrary to usual devices, it is possible, with a dense network of spatially distributed sensors, to analyze easily several environmental factors. However, the presented method only provides a yes/no information about runoff occurrence and does not allow a direct measure of surface runoff volume. The latter can be estimated indirectly using field

parameters coupling with equations such as Green and Ampt (1911) or Smith and Parlange equation (1978).

Results presented in this paper open interesting perspectives for extensive use of simple field measurements based on easy to implement sensors for surface runoff detection. It may contribute to an enhanced understanding of hydrological processes dynamics. Such observation network can be used more widely for example for hydrological models calibration and evaluation.

Perspectives: towards a holistic observation of surface runoff in a catchment?

As part of the AVuPUR project, several water level sensors were installed (Sarrazin, 2012) in temporary river of the observation catchment presented above. These sensors were used to investigate hydrological response in these rivers after rainfall events and evaluate the spatial extension of the drainage network. The recorded time series allowed derivation of several indices related to water cycle dynamics in these river reaches. The observation method presented in this paper provides a description of surface runoff in the catchment hillslopes connected to temporary river reaches. Coupling this method with the water level sensor monitoring in river reaches, may allow improving knowledge of surface water dynamics in a given catchment. Fig. 1 shows the locations of the water level sensors and that of the soil water content sensors. The spatial distribution of such an observation system would allow a full description of surface runoff dynamics in the catchment. On catchment with areas sensitive to surface runoff, the first and fast peaks in rivers are generally linked to surface runoff because it's a fast hydrological process.

Fig. 19 compares the first soil horizon water content (site #6) and the water level time series recorded in the intermittent river reach located downstream the same hillslope (site #a). The elapsed time between the onset of rainfall and the occurrence of surface runoff was estimated and is about 3 hours. The elapsed time between the onset of rainfall and the observed water level peak is 35 minutes. It can be compared to a kinematic wave based transfer time along the surface runoff transfer paths depicted by the IRIP method. The flow in the temporary river has probably multiple origins. Since it occurs after the peak of the generated surface runoff, it is however probably linked to the surface runoff generation upstream.

This kind of instrumentation would not be relevant in contexts where subsurface flow and groundwater may influence surface runoff dynamics, nor for catchment with long response times. This observation method, coupling hillslope observation and measures in river may allow investigating characteristic times of surface runoff from upstream to downstream in a whole catchment as demonstrated in Fig. 19. It may also open perspectives for surface runoff processes description, monitoring and modeling.

Many applications can be derived from this observation method such as models calibration and validation by describing catchment characteristic times. Another application may be related to flash floods monitoring or prevention. Indeed, it could be possible to calibrate a flash flood monitoring system by combining a surface runoff susceptibility map and holistic observation devices.

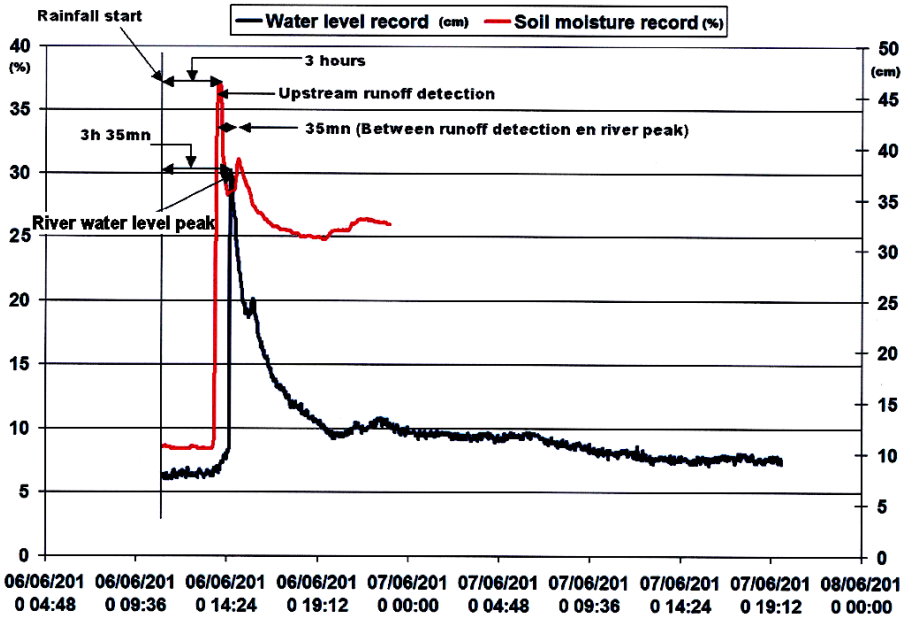

Fig. 19: Characteristic times for a catchment overland flow using soil surface water content data (site #6) and a water level sensor in the closest river stream at site #a on Fig. 1

Acknowledgements

We thank the *Rhône-Alpes Region* and Water Agency (*Agence de l'Eau Rhône-Méditerrannée & Corse*) for funding the project. Thanks to Irstea technical team (French National Research Institute of Science and Technology for Environment and Agriculture) for help in sensors installation and maintenance. We thank the *GRAIE* association, *Grand-Lyon* metropolitan city authorities, the governmental agency *DREAL Rhône* and INSA and INRA research centers for their participation in the program. We thank residents of the Mercier catchments who authorized sensors installation. AVuPUR (Assessing the Vulnerability of Peri-Urban Rivers) project, funded by the French Research Agency (ANR) under contract ANR-07-VULN-01, provided some of data used in this study. We also thank the French Railway Company SNCF for its interest in continuing the IRIP method development with the IRIP Rail project that funds the development of the iRIP software, and its implementation for the French railway network.

References

Abudi, I., Carmi, G., Berliner, P., 2012. Rainfall simulator for field runoff studies. Journal of Hydrology, 454–455(0): 76-81.

Arnaez, J., Lasanta, T., Ruiz-Flaño, P., Ortigosa, L., 2007. Factors affecting runoff and erosion under simulated rainfall in Mediterranean vineyards. Soil and Tillage Research, 93(2): 324-334.

Assouline, S., Ben-Hur, M., 2006. Effects of rainfall intensity and slope gradient on the dynamics of interrill erosion during soil surface sealing. CATENA, 66(3): 211-220.

Badoux, A., Witzig, J., Germann, P.F., Kienholz, H., Lüscher, P., Weingartner, R., Hegg, C., 2006. Investigations on the runoff generation at the profile and plot scales, Swiss Emmental. Hydrological Processes, 20(2): 377-394.

Beven, K.J., 2006. Streamflow Generation Processes. IAHS, ISBN Number: 978-1-901502-53-4(Publication Number: BM1): 432.

Blanco-Canqui, H., Gantzer, C.J., Anderson, S.H., Alberts, E.E., Ghidey, F., 2002. Saturated Hydraulic Conductivity And Its Impact On Simulated Runoff For Claypan Soils. Soil Sci. Soc. Am. J., 66(5): 1596-1602.

Boughton, W., Droop, O., 2003. Continuous simulation for design flood estimation—a review. Environmental Modelling & Software, 18(4): 309-318.

Braud, I., Breil, P., Thollet, F., Lagouy, M., Branger, F., Jacqueminet, C., Kermadi, S., Michel, K., 2013. Evidence of the impact of urbanization on the hydrological regime of a medium-sized periurban catchment in France. Journal of Hydrology, 485: 5-23.

Braud, I., Chancibault, K., Debionne, S., Lipeme Kouyi, G., Sarrazin, B., Jacqueminet, C., Andrieu, H., Béal, D., Bocher, E., Boutaghane, H. et al., 2010. The AVuPUR project (Assessing the Vulnerabiliy of Peri-Urbans Rivers): experimental set up, modelling strategy and first results, 7th Novatech 2010 Conference June 28-July 1 2010, Lyon, France, pp. 10 p.

Braud, I., Vich, A., Zuluaga, J., Fornero, L., Pedrani, A., 2001. Vegetation influence on runoff and sediment yield in the Andes region: observation and modelling. Journal of Hydrology, 254: 124-144.

Bryan, R.B., 2000. Soil erodibility and processes of water erosion on hillslope. Geomorphology, 32(3–4): 385-415.

Carey, W.P., Simon, A., 1984. Physical basis and potential estimation techniques for soil erosion parameters in the Precipitation-Runoff Modeling System. U.S. Geol. Surv. Water-Resour. Invest. Rep.: 84-4218.

Castillo, V.M., Gomez-Plaza, A., Martinez-Mena, M., 2003. The role of antecedent soil water content in the runoff response of semiarid catchments: a simulation approach. Journal of Hydrology, 284(1-4): 114-130.

Chanasyk, D.S., Mapfumo, E., Willms, W., 2003. Quantification and simulation of surface runoff from fescue grassland watersheds. Agricultural Water Management, 59(2): 137-153.

Connolly, R.D., Ciesiolka, C.A.A., Silburn, D.M., Caroll, C., 1997. Distributed parameter hydrology model (ANSWERS) applied to a range of catchment scales using rainfall simulator data IV: Evaluating pasture catchment hydrology. Journal of Hydrology, 201: 311-328.

Connolly, R.D., Silburn, D.M., 1995. Distributed parameter hydrology model (ANSWERS) applied to a range of catchment scales using rainfall simulator data II: Application to spatially uniform catchments. Journal of Hydrology, 172: 105-125.

de Jong van Lier, Q., Sparovek, G., Flanagan, D.C., Bloem, E.M., Schnug, E., 2005. Runoff mapping using WEPP erosion model and GIS tools. Computers & Geosciences, 31(10): 1270-1276.

de Lavenne, A., 2010. Risque d'inondation par ruissellement: Instrumentation terrain et analyse géomatique. Rapport de stage Ingénieur. Agroscampus Ouest/ ESA d'Angers: 95p.

De Roo, A.P.J., Offermans, R.J.E., Cremers, N.H.D.T., 1996a. Lisem: a single-event, physically based hydrological and soil erosion model for drainage basins. II: sensitivity analysis, validation and application. Hydrological Processes, 10(8): 1119-1126.

De Roo, A.P.J., Wesseling, C.G., Ritsema, C.J., 1996b. Lisem: a single-event physically based hydrological and soil erosion model for drainage basins. I: theory, input and output. Hydrological Processes, 10(8): 1107-1117.

Dehotin, J., Breil, P., 2011a. Rapport bibliographique: Cartographie de l'aléa inondation par ruissellement. Document de synthèse Projet IRIP: 35p.

Dehotin, J., Breil, P., 2011b. Rapport technique du projet IRIP : Cartographie de l'aléa inondation par ruissellement, Cemagref-Publications.

Dekker, L., Ritsema, C., 2000. Wetting patterns and moisture variability in water repellent Dutch soils. Journal of Hydrology, 231-232(0): 148-164.

DHI, 2002. Soil Erosion Assessment using GIS Version 1.0 Documentation and User Guide SEAGIS. DANISH HYDRAULIC INSTITUTE (DHI) WATER AND ENVIRONMENT Horsholm, Denmark, DHI: 23 p.

Douvinet, J., Delahaye, D., Langlois, P., 2006. Application of cellular automata modelling to analyse the dynamics of hyper-concentrated stream flows on loamy plateau (Paris Basin, North-West France). In: Ph. Gourbesville, J.C., V. Guinot and S.Y. Liong (Eds) (Ed.), 7th International Conference on Hydroinformatics. Reserach Publishing, Nice, France, pp. 1042-1055.

Dunjó, G., Pardini, G., Gispert, M., 2004. The role of land use–land cover on runoff generation and sediment yield at a microplot scale, in a small Mediterranean catchment. Journal of Arid Environments, 57(2): 239-256.

Dunne, T., Black, R.D., 1970. An Experimental Investigation of Runoff Production in Permeable Soils. Water Resour. Res., 6(2): 478-490.

Dunne, T., Moore, T., Taylor, C., 1975. Recognition and prediction of runoff-producing zones in humid regions.

Dunne, T., Zhang, W., Aubry, B.F., 1991. Effects of rainfall, vegetation, and microtopography on infiltration and runoff. Water Resources Research, 29(9): 2271-2285.

Dutton, A.L., Loague, K., Wemple, B.C., 2005. Simulated effect of a forest road on near-surface hydrologic response and slope stability. Earth Surface Processes and Landforms, 30: 325-338.

El Kateb, H., Zhang, H., Zhang, P., Mosandl, R., 2013. Soil erosion and surface runoff on different vegetation covers and slope gradients: A field experiment in Southern Shaanxi Province, China. CATENA, 105(0): 1-10.

Gonzalez-Sosa, E., Braud, I., Dehotin, J., Lassabatère, L., Angulo-Jaramillo, R., Lagouy, M., Branger, F., Jacqueminet, C., Kermadi, S., Michel, K., 2010. Impact of land use on the hydraulic properties of the topsoil in a small French catchment. Hydrological Processes, 24(17): 2382-2399.

Govers, G., Loch, R.J., 1993. Effects of initial water content and soil mechanical strength on the runoff erosion resistance of clay soils. Soil Research, 31(5): 549-566.

Graham, C.B., Woods, R.A., McDonnell, J.J., 2010. Hillslope threshold response to rainfall: (1) A field based forensic approach. Journal of Hydrology, 393(1–2): 65-76.

Green, W.H., Ampt, G., 1911. Studies of soil physics, Part I- The flow of air and water through soils. J. Ag. Sci., 4: 1-24.

Harbor, J.M., 1994. A Practical Method for Estimating the Impact of Land-Use Change on Surface Runoff, Groundwater Recharge and Wetland Hydrology. Journal of the American Planning Association, 60(1): 95-108.

Hartanto, H., Prabhu, R., Widayat, A.S.E., Asdak, C., 2003. Factors affecting runoff and soil erosion: plot-level soil loss monitoring for assessing sustainability of forest management. Forest Ecology and Management, 180(1-3): 361-374.

Hino, M., Odaka, Y., Nadaoka, K., Sato, A., 1988. Effect of initial soil moisture content on the vertical infiltration process - A guide to the problem of runoff-ratio and loss. Journal of Hydrology, 102(1â€“4): 267-284.

Holzmann, H., Sereinig, N., 1997. In situ measurements of hillslope runoff components with different types of forest vegetation. International Association of Hydrological Sciences, Wallingford, ROYAUME-UNI, IX, 363 p. pp.

Horton, R.E., 1945. Erosional development of streams and their drainage basins; hydrophysical approach to quantitative morphology. Geological Society of America Bulletin, 56(3): 275-370.

Huang, C., Gascuel-Odoux, C., Cros-Cayot, S., 2002. Hillslope topographic and hydrologic effects on overland flow and erosion. CATENA, 46(2-3): 177-188.

Hudson, N.W., 1993. Field measurement of soil erosion and runoff. Food and Agriculture Organization of the United Nations, 68.

Jacqueminet, C., Kermadi, S., Michel, K., Béal, D., Branger, F., Jankowsky, S., Braud, I., 2013. Land cover mapping using aerial and VHR satellite images for distributed hydrological modelling of periurban catchments: application to the Yzeron catchment (Lyon, France). Journal of Hydrology, 485(68-83).

Jain, M.K., Singh, V.P., 2005. DEM-based modelling of surface runoff using diffusion wave equation. Journal of Hydrology, 302(1-4): 107-126.

Koutroulis, A.G., Tsanis, I.K., 2010. A method for estimating flash flood peak discharge in a poorly gauged basin: Case study for the 13–14 January 1994 flood, Giofiros basin, Crete, Greece. Journal of Hydrology, 385(1-4): 150-164.

Lafforgue, A., 1977. Inventaire et examen des processus élémentaires de ruissellement et d'infiltration sur parcelles: Application à une exploitation méthodique des données obtenues sous pluies simulées. Cahiers de l'ORSTOM, Sér hydrol, XIV(4).

Lange, J., Haensler, A., 2012. Runoff generation following a prolonged dry period. Journal of Hydrology, 464–465(0): 157-164.

Langlois, P., Delahaye, D., 2002. RuiCells, automate cellulaire pour la simulation du ruissellement de surface. Revue Internationale de Géomatique, 12(4): 461-487.

Latron, J., Gallart, F., 2008. Runoff generation processes in a small Mediterranean research catchment (Vallcebre, Eastern Pyrenees). Journal of Hydrology, 358(3–4): 206-220.

Le Bissonnais, Y., Montier, C., Daroussin, J., King, D., 1998. Cartographie de l'aléa Erosion des sols en France. IFEN Collection Etudes et Travaux, 18.

Le Bissonnais, Y., Renaux, B., Delouche, H., 1995. Interactions between soil properties and moisture content in crust formation, runoff and interrill erosion from tilled loess soils. CATENA, 25(1-4): 33-46.

Le Gouée, P., Delahaye, D., 2008. Modélisation et cartographie de l'aléa érosion des sols et des espaces de ruissellement dans le Calvados. Rapport d'étude.

Lê, S., Josse, J., Husson , F., Mazet, J., 2008. FactoMineR: An R Package for Multivariate Analysis. Journal of Statistical Software, 25(1).

Muñoz-Villers, L.E., McDonnell, J.J., 2012. Runoff generation in a steep, tropical montane cloud forest catchment on permeable volcanic substrate. Water Resources Research, 48(9): W09528.

Navas, A., Alberto, F., Machín, J., Galán, A., 1990. Design and operation of a rainfall simulator for field studies of runoff and soil erosion. Soil Technology, 3(4): 385-397.

Nearing, M.A., Foster, G.R., Lane, L.J., Finkner, S.C., 1989. A process-based soil erosion model for USDA-water erosion prediction project technology. ASABE (American Society of Agricultural and Biological Engineers), 32(5): 1587-1593.

Nicolas, M., 2010. Etude expérimentale et numérique du ruissellement de surface : effets des variations d'intensité de la pluie. Application à une parcelle de vigne en Cévennes-Vivarais. Thèse de doctorat, LTHE - Université joseph Fourier. Grenoble.

Pagès, J., 2004. Analyse factorielle de données mixtes. Revue de Statistique Appliquée: 93-111.

Pérez-Latorre, F.J., de Castro, L., Delgado, A., 2010. A comparison of two variable intensity rainfall simulators for runoff studies. Soil and Tillage Research, 107(1): 11-16.

Peters, D., Buttle, J., Taylor, C., LaZerte, B., 1995. Runoff production in a forested, shallow soil, Canadian Shield basin Water Resources Research, 31(5): 291-1304.

Power, J.F., Sandoval, F.M., Ries, R.E., Merrill, S.D., 1980. Effects of Topsoil and Subsoil Thickness on Soil Water Content and Crop Production on a Disturbed Soil. Soil Sci. Soc. Am. J., 45(1): 124-129.

Rahimy, P., 2012. Effects of Soil Depth Spatial Variation on Runoff Simulation, Using the Limburg Soil Erosion Model (LISEM), a Case Study in Faucon Catchment, France. Soil and Water Research, 7(2): 52–63.

Renard, K.G., Foster, G.R., Weesies, G.A., Porter, J.P., 1991. RUSLE: Revised universal soil loss equation. Journal of Soil and Water Conservation, 46(1): 30-33.

Rice, K.C., Hornberger, G.M., 1998. Comparison of hydrochemical tracers to estimate source contributions to peak flow in a small, forested headwater catchment. Wat. Resour. Res, 34: 1755-1766.

Roose, E., 1977. Erosion et ruissellement en Afrique de l'Ouest, vingt années de mesures en parcelles expérimentales. ORSTOM, pp. 104.

Roose, E., ARABI, M., BRAHAMIA, K., CHEBBANI, R., MAZOUR MORSLI, B., 1993. Erosion en nappe et ruissellement en montagne mediterranéenne algérienne : Réduction des risques érosifs et intensification de la production agricole par la GCES : synthèse des campagnes 1984-1995 sur un réseau de 50 parcelles d'érosion. ORSTOM, Bondy, FRANCE, 275 pp.

Sarrazin, B., 2012. MNT et observations multi-locales du réseau hydrogranphique d'un petit bassin versant rural dans une perspective d'aide à la modélisation hydrologique. Ecole doctorale Terre, Univers, Environnement. l'Institut National Polytechnique de Grenoble.: 269 pp.

Schmocker-Fackel, P., Naef, F., Scherrer, S., 2007. Identifying runoff processes on the plot and catchment scale. Hydrol. Earth Syst. Sci., 11(2): 891-906.

Sharpley, A.N., 1985. Depth of surface soil-runoff interaction as affected by rain fall, soil slope, and management. Journal - Soil Science Society of America July/Aug, 49(4).

Silva, C.L., Oliveira, C.A.S., 1999. Runoff measurement and prediction for a watershed under natural vegetation in Central Brazil, 23. Sociedade Brasileira de Ciência do Solo, Campinas, BRESIL.

Singh, R., Panigrahy, N., Philip, G., 1999. Modified rainfall simulator infiltrometer for infiltration, runoff and erosion studies. Agricultural Water Management, 41(3): 167-175.

SIRA, 2012. Cartographie des sols du Rhone: Application à la réalisation de cartes d'aptitudes culturales et forestières et à l'étude de l'enracinement de la vigne du Beaujolais. Ministère de l'Agriculture: Programme Inventaire, Gestion et Conservation des Sols (IGCS). Chambre d'Agriculture du Rhône: 75.

Smith, M.B., Seo, D.-J., Koren, V.I., Reed, S.M., Zhang, Z., Duan, Q., Moreda, F., Cong, S., 2004. The distributed model intercomparison project (DMIP): motivation and experiment design. Journal of Hydrology, 298(1-4): 4-26.

Smith, R.E., 2002. Infiltration Theory for Hydrologic Applications. Water Resources Monograph 15, American Geophysical Union, Washington, DC.

Smith, R.E., Goodrich, D.C., Woolhiser, D.A., Unkrich, C.L., 1995. KINEROS: A Kinematic Runoff and Erosion Model, chap. 20 of Computer Models of Watershed Hydrology, (Ed. by Singh, V. J.). Water Resour. Pub Highlands Ranch, Colo: 697-732.

Smith, R.E., Parlange, J.Y., 1978. A parameter-efficient hydrologic infiltration model. Water Resources Research, 14(3): 533-538.

Truman, C.C., Potter, T.L., Nuti, R.C., Franklin, D.H., Bosch, D.D., Antecedent water content effects on runoff and sediment yields from two Coastal Plain Ultisols. Agricultural Water Management, 98(8): 1189-1196.

Weiler, M, Scherrer, S, Naef, F, Burlando, P, 1999. Hydrograph separation of runoff components based on measuring hydraulic state variables, tracer experiments, and weighting methods. International Association of Hydrological Sciences, Wallingford, ROYAUME-UNI, IX, 284 p. pp.

Wemple, B.C., Jones, A.J., 2003. Runoff production on forest roads in a steep, mountain catchment. Water Resources Research, 39(8): 1220, doi: 10.1029/2002WR001744.

Woolhiser D.A., Smith R.E., D.C., G., 1990. KINEROS - A kinematic runoff and erosion model, documentation and user manual. . USDA, ARS: 130.

Wu, T., Hall, J., Bonta, J., 1993. Evaluation of Runoff and Erosion Models. Journal of Irrigation and Drainage Engineering, 119(2): 364-382.